

Online Optimal Mode Control for Plug-in Hybrid Vehicles Based on Driving Routes

Ryunosuke Watanabe* Hiroto Yoshioka** Tatsuya Ibuki*
Yoshihiro Sakayanagi*** Mitsuji Sampei*

* *Tokyo Institute of Technology, Tokyo, Japan*
(*e-mail: rwata@sl.sc.e.titech.ac.jp, {ibuki, sampei}@sc.e.titech.ac.jp*)
** *NSK Ltd., Tokyo, Japan (e-mail: yoshioka@sl.sc.e.titech.ac.jp)*
*** *Toyota Motor Corporation, Shizuoka, Japan*
(*e-mail: yoshihiro_sakayanagi@mail.toyota.co.jp*)

Abstract:

This paper proposes an online optimal mode control method to minimize fuel consumption for plug-in hybrid vehicles (PHVs) considering two drive modes: electric vehicle (EV) and hybrid vehicle (HV) modes. The proposed method predicts fuel and electricity consumption of PHVs based mainly on a driving-route model that considers road grades and vehicle speed distributions. The driving-route model is estimated with terrain maps and historical driving data on a planned route. In this work, two energy consumption maps are built for the EV and HV modes of the PHVs. The driving-route model and energy consumption maps lead to the formulation of an integer linear programming problem by regarding the two drive modes as binary variables. A detailed vehicle simulator, called ADVISOR, demonstrates that the proposed method improves fuel efficiency over that of a conventional method.

Keywords: Plug-in Hybrid Vehicles; Energy Management Systems; Integer Programming; Online Control; Statistical Analysis; Stochastic Systems

1. INTRODUCTION

Optimal energy management for systems with two or more resources is essential to improve operational efficiency. This is because these various resources have distinct advantages and disadvantages (e.g., peak energy-conversion efficiency). A typical example of such systems is plug-in hybrid vehicles (PHVs). PHVs have two energy resources: fuel and electricity. Each resource generates torque via an engine, a battery, a motor, a generator, and gears. These processes cause different types of energy loss depending on driving conditions, such as road grade, speed, and weather. Therefore, PHVs require higher-level energy management considering driving conditions to achieve efficient driving than vehicles with a single resource. Many strategies have been proposed previously (see Wirasingha and Emadi (2011); Torres et al. (2014); Sun et al. (2015)).

More recently, strategies using statistical information about driver behaviors and driving cycles have attracted interest in the hybrid automotive industry. Moura et al. (2011) provide a stochastic optimal control approach to build a static feedback map offline. The static feedback map can be processed in real time on an actual PHV. Sun et al. (2015) achieve near-optimal fuel consumption using a traffic data-enabled predictive control framework. Kelly et al. (2012) propose a charging strategy focusing on ways in which driving patterns and demographics affect energy consumption. Ripaccioli et al. (2010) and Cairano et al. (2014) develop an approach for driver-aware vehicle control based on stochastic model predictive control (SMPC)

with learning. This framework combines a Markov chain representation of driver behavior, scenario-based stochastic optimization, and quadratic programming. Malikopoulos (2013) addresses the optimization problem of online supervisory control in a hybrid electric vehicle (HEV). The HEV operation is modeled as a controlled Markov chain and treats the supervisory control as a dual constrained optimization problem.

However, the main focus of the prior work is to determine how the actions of each driver impact the vehicle model. To the best of the authors' knowledge, there exist no studies that attempt to adopt vehicle speed distributions on driving routes as stochastic modeling for an optimal energy strategy. In addition, Chau et al. (2017) point out that the aforementioned results often assume complete control of internal energy management systems in PHVs. Following that research, this paper discusses the optimal control of drive modes, which are among the configuration options to achieve efficient driving and are described in Section 2.

To tackle these issues, this work focuses on modeling driving routes and proposes an online optimal mode-control method to minimize fuel consumption for PHVs. The driving-route model is built with road grades and vehicle speed distributions. These are estimated from terrain maps and historical driving data, i.e., statistical information, on a planned route. In this research, two energy consumption maps are also built for the drive modes of PHVs as a vehicle model. From the driving-route model and energy consumption maps, the energy demand of the planned course can

be predicted. As a result, the online optimal mode control can be formulated as an integer linear programming (ILP) problem with the drive modes, fuel consumption, and electricity limitations as the decision variables, cost function, and constraints, respectively. The ILP problem is computationally tractable, unlike general mixed-integer programming problems. This computational tractability is demonstrated by the numerical simulation results. The simulation results also show that the proposed method improves fuel efficiency over the conventional method. Another advantage of this method is that any PHVs can share and use the driving route information. In the case of driver-aware control, it is difficult to accurately convert driver-behavior data to another PHV, as the data are personalized.

The rest of this paper is organized as follows. Section 2 describes the problem settings of this study, energy consumption maps, and modeling the driving route. Section 3 proposes the online optimal mode-control method and provides the formulation of the ILP problem. A theoretical property of the method's constraints is also discussed. Section 4 shows the simulation results of the proposed approach via a detailed numerical simulator (ADVISOR, see Brooker et al. (2013); Markel et al. (2002)). The simulation results indicate that the present method can improve fuel efficiency compared with the conventional method. Section 5 summarizes the conclusions.

2. PROBLEM SETTINGS AND MODELING

2.1 Problem Settings

We consider a model of the driving route shown in Fig. 1. This model is a finite route that has a departure and an arrival place. The route is discretized by a sampling distance d . Each sampling distance interval is numbered as $1, \dots, N$. $\theta^1, \dots, \theta^N$ denotes the road grades, and v^1, \dots, v^N and V^1, \dots, V^N denote the realizations and random variables of the vehicle speed at each distance interval, respectively.

This paper imposes the following assumptions:

Assumption 1. A driving route is defined in advance, e.g., a commuting route or other driving route searched by navigation systems.

Assumption 2. The road grades $\theta^1, \dots, \theta^N$ are deterministic variables, and they can be collected from databases such as Global Positioning Systems and 3-D terrain maps (Sun et al. (2015)). The vehicle speeds V^1, \dots, V^N are discrete random variables with possible values v_1, \dots, v_{n_v} and follow discrete conditional probability distributions with the Markov property. Thus, we can obtain a discrete conditional probability distribution of

$$\Pr(V^k | V^{k-1}, V^{k-2}, \dots, V^1) = \Pr(V^k | V^{k-1}).$$

In addition, the probability distribution of the initial interval $\Pr(V^1)$ is given.

Assumption 3. At the current distance interval $k \in \{1, \dots, N-1\}$, the realized vehicle speed $v^k \in \{v_1, \dots, v_{n_v}\}$ and state of charge (SoC) of the battery $SoC^k \in [0, 1]$ are known.

In this study, the control input is the drive mode at each distance interval. The drive modes are classified into two

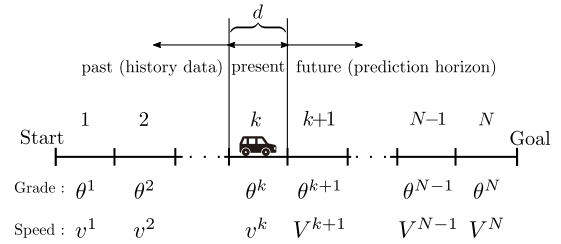


Fig. 1. Modeling the driving route: d is the sampling distance interval, θ^k is the road grade, and v^k and V^k are the realization and random variable of vehicle speed.

Table 1. Battery specifications of Prius PHV (Toyota Motor Corporation (2016))

Cell voltage	3.7 V	Total voltage	207.2 V
Cell capacity	21.5 Ah	Total capacity	4.4 kWh
Number of cells	56		

types. The first is the electric vehicle (EV) or charge-depleting (CD) mode. In this mode, PHVs use only the electricity resource. The other is called hybrid vehicle (HV) or charge-sustaining (CS) mode. In this mode, PHVs generate the driving force with fuel, electricity, or both while maintaining a constant SoC of the battery.

The PHVs currently on the market have adopted a rule-based strategy, named the CDCS method (Wirasingha and Emadi (2011)). The CDCS method follows a simple set of rules: i) depleting the electricity from the battery in the CD mode and ii) consuming the fuel to travel the remaining distance in the CS mode. This conventional method is suboptimal when the trip distance exceeds the all-electric range, as it does not consider driving conditions (Pisu and Rizzoni (2007)). Unlike the conventional method, the proposed method optimizes EV–HV mode switching to reduce fuel consumption.

2.2 Modeling of PHV with Energy Consumption Map

In this section, two energy consumption maps are built to compute the fuel and electricity used by the PHVs in the HV and EV modes. Suppose that the effects of the road grade and vehicle speed on the energy consumption on the entire trip are sufficiently large compared to the other impacts, including inertia. In addition, assume that the energy obtained by regenerative brakes is used to re-accelerate PHVs. The simulation results in Section 4 indicate that these assumptions are reasonable¹.

Figure 2 shows: (a) fuel energy consumption map $w_f(\theta, v)$ and (b) electric energy consumption map $w_e(\theta, v)$. These maps depict the average energy consumption when a PHV model runs on a road with grade θ at speed v , where the road grade ranges from -6% to 6% in increments of 1% and the speed ranges from 5 km/h to 100 km/h in increments of 5 km/h. This paper uses a Prius model in ADVISOR to create these two maps. Some specifications of the batteries are adjusted to those of the Prius PHV from Toyota Motor Corporation (2016), as enumerated in Table 1.

¹ Note that inertia is another critical factor regarding instantaneous energy consumption if the vehicle is accelerating or decelerating.

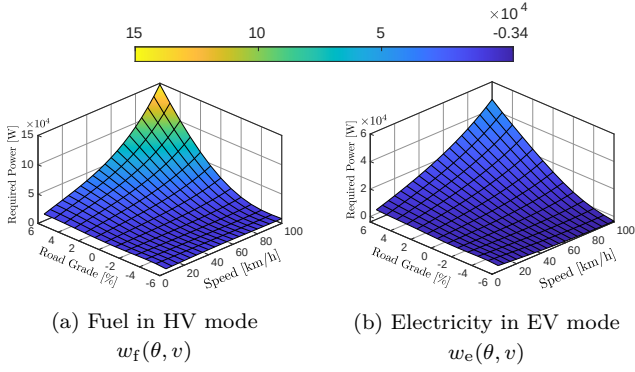


Fig. 2. Modeling PHV as two energy consumption maps obtained by detailed numerical simulation

2.3 Stochastic Modeling of Vehicle Speed

Based on Assumption 2, this section introduces the transition probability matrices of the vehicle speed for each sampling distance interval as follows:

$$P^k = [p_{ab}^k], p_{ab}^k = \Pr(V^{k+1} = v_b \mid V^k = v_a), \quad (1)$$

where $k \in \{1, \dots, N-1\}$, $a, b \in \{1, \dots, n_v\}$, $\sum_b p_{ab}^k = 1$. These transition probabilities can be estimated from known cycles, such as past driving data and standard driving cycles. This work estimates the transition probabilities p_{ab}^k from historical driving cycles. The estimation is a simple method based on Nadaraya–Watson kernel regression (Nadaraya (1964); Watson (1964); Tamaki et al. (2014)). Figure 3a shows an example of the estimated transition probability matrices of the vehicle speed from interval step k to $k+1$.

These transition probability matrices are estimated for each driving route against the driver-aware control (Ripaccioli et al. (2010); Cairano et al. (2014)). Therefore, all PHVs can share the driving records even if their powertrain properties are different. Note that, however, the driving records on each route require large data storage.

Using the estimated transition probabilities (1), the proposed method computes the probability distributions of the vehicle's speed throughout the planned route. Suppose the probability distribution of the initial interval $\Pr(V^1)$ and the realization v^k are known by Assumption 3. Then, we can calculate the probability distributions for each interval from $k+1$ to N as

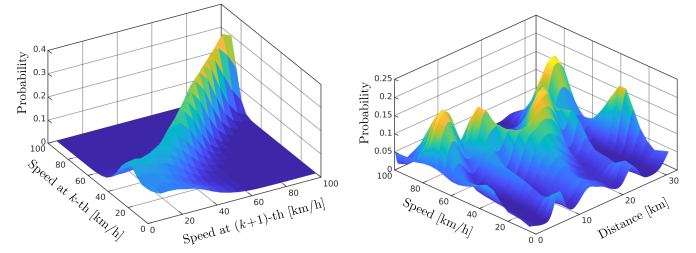
$$\Pr(V^i) = \Pr(V^{i-1}) P^{i-1}, \quad i \in \{k+1, \dots, N\}, \quad (2)$$

where, $\Pr(V^i) = [\Pr(V^i = v_1) \dots \Pr(V^i = v_{n_v})]$, $\Pr(V^k) = [\mathbb{I}(v^k = v_1) \dots \mathbb{I}(v^k = v_{n_v})]$, and the Markov property is used to obtain (2). $\mathbb{I}(\cdot)$ is the indicator function of (\cdot) , taking a value of 1 if (\cdot) is true and 0 otherwise. Figure 3b shows an example of the probability distributions from the initial to final intervals on the driving route.

3. ONLINE OPTIMAL MODE CONTROL

3.1 Problem Formulation

The present method aims to minimize fuel consumption while handling the electricity constraint of PHVs. This paper formulates an optimization problem with constraints using the basic concepts of SMPC (Mesbah (2016)).



(a) Estimated transition probability matrix of vehicle speed from interval k to $k+1$ (b) Probability distributions of vehicle speed throughout a trip from interval k to $k+1$

Fig. 3. Stochastic modeling of vehicle speed on one driving route. The sampling distance intervals range from 0 km to 32.1 km at increments of 0.1 km.

Let $k \in \{1, \dots, N-1\}$ be the current distance interval on the driving route. We consider the following cost function:

$$J^k = \mathbf{E} \left[\sum_{i=k+1}^N \Delta w_f(\theta^i, V^i) (1 - u^i) \mid v^k \right] \quad (3)$$

with respect to an open-loop mode control input sequence $u^i \in \{0, 1\}$, where $\Delta w_f(\theta^i, V^i) = w_f(\theta^i, V^i) d/V^i$. u^i denotes the EV–HV mode switching (1: EV mode, 0: HV mode); it uses zero-order approximation during each sampling distance step. $\Delta w_f(\theta^i, V^i)$ denotes the fuel energy consumption with distance d for each interval. $\mathbf{E}[\cdot \mid v^k]$ is the conditional expected value operator for the realization of the vehicle speed v^k at the current step k . The cost function (3) can be calculated as

$$\begin{aligned} J^k &= \mathbf{E} [\Delta w_f(\theta^{k+1}, V^{k+1}) (1 - u^{k+1}) + \dots \\ &\quad \dots + \mathbf{E} [\Delta w_f(\theta^N, V^N) (1 - u^N) \mid v^k] \dots \mid v^k] \\ &= \sum_{i=k+1}^N \sum_{b=1}^{n_v} \Pr(V^i = v_b) \Delta w_f(\theta^i, v_b) (1 - u^i) \end{aligned} \quad (4)$$

using (2). The cost function (3) means that the expected values of fuel consumption are accumulated for the intervals in which the PHV is in the HV mode.

This optimization problem minimizes (3) subject to the following constraints of the electricity resource:

$$SoC_{\min} \leq SoC_\ell \leq SoC_{\max}, \quad \ell \in \{k+1, \dots, N\}, \quad (5)$$

where SoC_{\min} and SoC_{\max} denote the lower and upper limitations of the SoC, respectively. The SoC limitations (5) are reformulated to

$$\mathbf{E} \left[\frac{1}{Q_{\text{full}}} \sum_{i=k+1}^{\ell} \Delta w_e(\theta^i, V^i) u^i - SoC_{\min}^k \mid v^k \right] \leq 0, \quad (6)$$

$$\mathbf{E} \left[-\frac{1}{Q_{\text{full}}} \sum_{i=k+1}^{\ell} \Delta w_e(\theta^i, V^i) u^i - SoC_{\max}^k \mid v^k \right] \leq 0, \quad (7)$$

where $\Delta w_e(\theta^i, V^i) = w_e(\theta^i, V^i) d/V^i$, $SoC_{\min}^k = SoC^k - SoC_{\min}$, $SoC_{\max}^k = SoC_{\max} - SoC^k$. SoC^k denotes the current SoC value, Q_{full} denotes the total electricity of the battery, and $\Delta w_e(\theta^i, V^i)$ denotes the electrical energy consumption with distance d for each interval. The inequality constraints (6), (7) can be represented, in the same way of (4), as

$$\frac{1}{Q_{\text{full}}} \sum_{i=k+1}^{\ell} \sum_{a=1}^{n_v} \Pr(V^i = v_a) \Delta w_e(\theta^i, v_a) u^i \leq \text{SoC}_{\text{min}}^k, \quad (8)$$

$$-\frac{1}{Q_{\text{full}}} \sum_{i=k+1}^{\ell} \sum_{a=1}^{n_v} \Pr(V^i = v_a) \Delta w_e(\theta^i, v_a) u^i \leq \text{SoC}_{\text{max}}^k \quad (9)$$

using (2).

In summary, the online optimal mode-control problem for the current step k is formulated as

$$(\mathcal{P}): \min_u (4) \text{ subject to } (8), (9),$$

where $u = [u^{k+1} \dots u^N]^T$ denotes the input sequence vector. Because (\mathcal{P}) is an ILP problem, it can be solved with standard ILP solvers. In this approach, the optimization problem (\mathcal{P}) is solved sequentially for each of the remaining intervals $k+1, \dots, N$. The PHV takes the first mode input $(u^*)^{k+1}$ for the next interval step.

The inequality constraints (6), (7) are not the chance constraint generally considered in SMPC. However, optimization problem (\mathcal{P}) implicitly provides a trade-off between the use of fuel and electricity in the process of solving the ILP problem. To express this trade-off as an ILP problem, the proposed approach imposes inequality constraints (6), (7) on the expected values of the SoC. A theoretical relationship between the constraints (6), (7) and the chance constraint is provided in Section 3.3.

3.2 Reduction of EV–HV Mode Switching Frequency

The solution to problem (\mathcal{P}) provides an optimal mode sequence vector. This optimal sequence of the drive modes allows the PHV to switch the EV–HV mode rapidly. This high-frequency mode switching can cause loss of drivability. In this section, to reduce the EV–HV mode switching frequency, a constraint is added to problem (\mathcal{P}) .

This study imposes the following equality constraint,

$$(c_{\text{eq}} - 1)u^{k+1} - (u^{k+2} + \dots + u^{k+c_{\text{eq}}}) = 0, \quad c_{\text{eq}} \in \{2, \dots, N - k\}, \quad (10)$$

in addition to the inequality constraints (8), (9). This equality constraint (10) implies that the same mode is used for intervals $k+1, \dots, k+c_{\text{eq}}$ in the optimization at step k . This statement also shows that it does not affect the computation cost, even if the total number of decision variables u increases. This paper defines problem (\mathcal{P}) with the mode-switching constraint (10) as

$$(\mathcal{Q}): \min_u (4) \text{ subject to } (8)–(10).$$

Because this optimization problem, (\mathcal{Q}) , is another ILP problem, the same solution scheme as (\mathcal{P}) can be used.

Note that the mode-switching constraint (10) does not guarantee that a given restricted input is also held for the optimization at the next step. Despite this, the solution of (\mathcal{Q}) can decrease the number of EV–HV mode switches compared to that of (\mathcal{P}) . One reason for this is that the optimal mode sequence of (\mathcal{Q}) may have an effect that differs from that of (\mathcal{P}) on the value of the SoC. This affected value of the SoC will induce an optimization result at the next step to keep the same drive mode.

3.3 Theoretical Property of (\mathcal{P}) in terms of Chance Constraint

This section describes a theoretical property of problem (\mathcal{P}) in terms of the chance constraint.

The following proposition shows that the inequality constraints (6), (7) on the expected value of the SoC depletion can be written as the chance constraint.

Proposition 4. Let $\hat{\theta}^t = (\theta^{k+1}, \dots, \theta^{k+t})$ and $\hat{V}^t = (V^{k+1}, \dots, V^{k+t})$, $t \in \{1, \dots, N - k\}$ be deterministic scenarios of the road grades and random scenarios of the vehicle speeds with all the possible realizations $\hat{v}^t = (v^{k+1}, \dots, v^{k+t})$, $v^{k+t} \in \{v_1, \dots, v_{n_v}\}$, respectively.

Assuming that $(u^*)^{k+t}$, $t \in \{1, \dots, N - k\}$ is the optimal solution of (\mathcal{P}) , the solution of (\mathcal{P}) has the following property related to a set of chance constraints:

$$\Pr(\{\hat{v}^t \mid \hat{v}^t \in \mathcal{C}_{\hat{v}^t}^+ \mid v^k\} \geq \max\left(\frac{\mathbf{E}[\Delta w_e^+(\hat{\theta}^t, \hat{V}^t) \mid v^k]}{Q_{\text{full}} \text{SoC}_{\text{min}}^k}, 0\right), \quad (11)$$

$$\Pr(\{\hat{v}^t \mid \hat{v}^t \in \mathcal{C}_{\hat{v}^t}^- \mid v^k\} \geq \max\left(\frac{-\mathbf{E}[\Delta w_e^-(\hat{\theta}^t, \hat{V}^t) \mid v^k]}{Q_{\text{full}} \text{SoC}_{\text{max}}^k}, 0\right), \quad (12)$$

where

$$w_e^+(\hat{\theta}^t, \hat{v}^t) = \mathbb{I}(\hat{v}^t \in \mathcal{C}_{\hat{v}^t}^+) \sum_{s=1}^t \Delta w_e(\theta^{k+s}, v^{k+s}) (u^*)^{k+s},$$

$$w_e^-(\hat{\theta}^t, \hat{v}^t) = \mathbb{I}(\hat{v}^t \in \mathcal{C}_{\hat{v}^t}^-) \sum_{s=1}^t \Delta w_e(\theta^{k+s}, v^{k+s}) (u^*)^{k+s},$$

$$\mathcal{C}_{\hat{v}^t}^+ = \left\{ \hat{v}^t \mid \frac{1}{Q_{\text{full}}} \sum_{s=1}^t \Delta w_e(\theta^{k+s}, v^{k+s}) (u^*)^{k+s} \leq \text{SoC}_{\text{min}}^k \right\},$$

$$\mathcal{C}_{\hat{v}^t}^- = \left\{ \hat{v}^t \mid -\frac{1}{Q_{\text{full}}} \sum_{s=1}^t \Delta w_e(\theta^{k+s}, v^{k+s}) (u^*)^{k+s} \leq \text{SoC}_{\text{max}}^k \right\}.$$

Proof. The proof is derived from (8), (9). \square

Proposition 4 implies that the chance constraints (11), (12) are defined depending only on the probability of the vehicle speed. This is because higher-order central moments (e.g., variance) are not considered (Farina et al. (2013); Hashimoto (2013)). The formulation of *risk-aware* constrained optimization that is physically meaningful to energy management for PHVs is an ongoing work. Although this theoretical limit to the constraints exists, the next section demonstrates that the proposed method can decrease fuel consumption compared to the CDCS method.

4. SIMULATION

This section shows the numerical simulation results of the proposed methods. These results are demonstrated via ADVISOR. The simulation uses `intlinprog` in MATLAB (MathWorks (2019)) as an ILP problem solver on a standard desktop computer. The desktop computer has Intel® Core™ i7-4790 3.60 GHz CPU and 16GB of RAM.

The simulation deals with a commuter driving on a real suburban route. The route has a total distance of

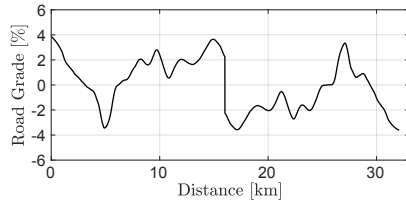


Fig. 4. Road grade profile of driving route for simulation

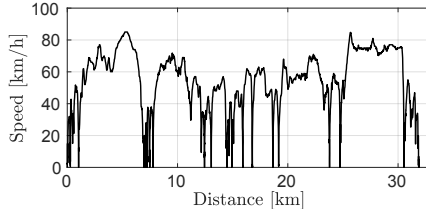


Fig. 5. Example of the vehicle speed profiles for estimation of probability distributions of speed

approximately 32.1 km and the road grades shown in Fig. 4. The transition probability matrices of this commute are estimated with 60 vehicle speed profiles, including approximately 19,000 data points recorded by DashCommand™ (Palmer Performance Engineering Corporation (2018)). Figure 5 illustrates an example of the vehicle speed profiles of the commute. As a PHV model, the two maps in Fig. 2 are used to compute the energy consumption.

This study prepares 500 real-cycle profiles that differ from the 60 cycles used for estimation. These additional profiles are used to verify whether the proposed method can improve the fuel consumption compared to that of the standard CDCS method. Note that *a priori* information is limited to the estimated transition probabilities of the vehicle speed, and the 500 driving profiles for the simulation are unknown.

4.1 Results in Case (P)

Figure 6 shows the performance results of the proposed method in case (P). It shows one example SoC profile, fuel consumption result, and input history. The proposed method schedules the switching in the first half of the route and sustains the electricity to travel parts of the last half in EV mode. Additionally, Table 2 summarizes the improvement ratio of the proposed methods to the CDCS method. It shows the average, standard deviation (SD), maximum, and minimum of verification via 500 drive cycles for each method. The average improvement in performance is 13.7%. The results shown in Fig. 6 and Table 2 indicate that the modeling of the driving route and the PHV is reasonable.

Problem (P) can be solved within 6 s on the standard desktop computer in most cases. A vehicle travelling at an average speed of 60 km/h for 0.1 km takes 6 s, which is longer than the computational time of the method. Hence, the online calculation for the actual PHVs can be processed on a standard- or high-performance machine (e.g., a cloud-computing server and high-performance control unit). The worst cases take approximately 10 s on average to solve the ILP problem, such cases occur only a few times in one trip. In these worst cases, the present method can alternatively use the second and subsequent inputs of the

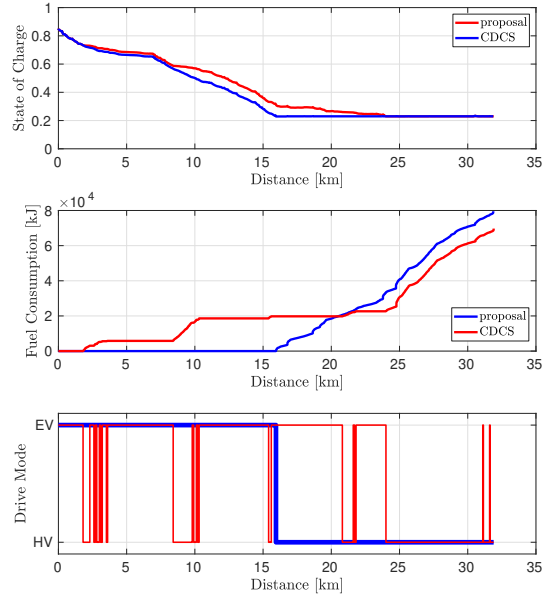


Fig. 6. Simulation results of one drive cycle via ADVISOR (proposal in case (P) vs. CDCS): The top, middle, and bottom are an SoC profile, accumulated fuel consumption result, and input history, respectively.

Table 2. Improvement ratio of fuel consumption w.r.t. CDCS method

	ave.	SD	max.	min.
Case (P)	13.7%	6.6%	30.7%	-3.3%
Case (Q)	11.1%	3.9%	24.9%	-0.4%

previous optimization result $(u^*)^{k+2}, (u^*)^{k+3}, \dots$ at the next step.

4.2 Results in Case (Q)

Figure 7 shows an example of the results in case (Q) with $c_{eq} = \min(5, N - k)$ to reduce the EV–HV mode switching frequency. Method (Q) can reduce the number of EV–HV mode switches compared to the result in Fig. 6c. The mode switching occurs 20.3 times on average in the case of Fig. 6c. In the case of Fig. 7c, the average number of mode switches is 11.9.

According to Table 2 in the case of (Q), the average improvement in performance is 11.1%. The computation time to solve problem (Q) is within 6 s in most cases. The efficiency and computation cost are nearly the same as those of case (P). Hence, method (Q) is helpful to optimize the energy consumption and reduce the EV–HV mode switching frequency simultaneously.

5. CONCLUSION

This paper discusses the online optimal mode control method for PHVs based on a driving-route model. In the proposed method, the driving-route model is estimated by statistical information, and the energy consumption maps of the PHV are built as two functions of the road grade and vehicle speed. These models are sequentially used in the ILP problem to determine the EV–HV mode to reduce fuel consumption. This approach is demonstrated

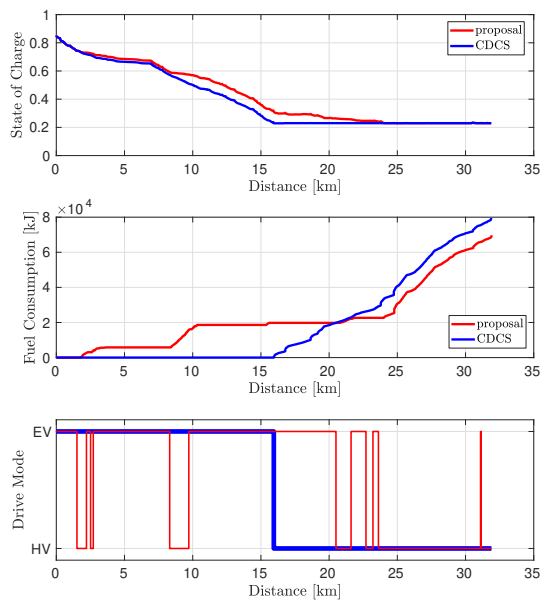


Fig. 7. Simulation results of one drive cycle via ADVISOR (proposal in case (Q) with $c_{eq} = \min(5, N - k)$ vs. CDCS): The top, middle, and bottom are an SoC profile, accumulated fuel consumption result, and input history, respectively.

in the detailed numerical simulator. The simulation results show that fuel consumption decreases compared with the conventional method, and the ILP problem can be solved in real time on a standard desktop computer.

As future work, implementation on an actual PHV and verification for many different driving scenarios are planned. We will also attempt to employ the variance values to a cost function and constraints to reduce variation in the improvement ratio.

REFERENCES

- Brooker, A., Haraldsson, K., Hendricks, T., Johnson, V., Kelly, K., Kramer, B., Markel, T., O’Keefe, M., Sprik, S., Wipke, K., Zolot, M., Bharathan, D., Burch, S., Cuddy, M., and Rausen, D. (2013). Advisor -advanced vehicle simulator-. <http://adv-vehicle-sim.sourceforge.net>. (accessed 9-Mar.-2020).
- Cairano, S.D., Bernardini, D., Bemporad, A., and Kolmanovsky, I.V. (2014). Stochastic mpc with learning for driver-predictive vehicle control and its application to hev energy management. *IEEE Transactions on Control Systems Technology*, 22(3), 1018–1031.
- Chau, C.K., Elbassioni, K., and Tseng, C.M. (2017). Drive mode optimization and path planning for plug-in hybrid electric vehicles. *IEEE Transactions on Intelligent Transportation Systems*, 18(12), 3421–3432.
- Farina, M., Giulioni, L., Magni, L., and Scattolini, R. (2013). A probabilistic approach to model predictive control. In *Proc. of the 2013 IEEE 52nd Annual Conference on Decision and Control*, 7734–7739.
- Hashimoto, T. (2013). Probabilistic constrained model predictive control for linear discrete-time systems with additive stochastic disturbances. In *Proc. of the 2013 IEEE 52nd Annual Conference on Decision and Control*, 6434–6439.
- Kelly, J.C., MacDonald, J.S., and Keoleian, G.A. (2012). Time-dependent plug-in hybrid electric vehicle charging based on national driving patterns and demographics. *Applied Energy*, 94, 395–405.
- Malikopoulos, A.A. (2013). Stochastic optimal control for series hybrid electric vehicles. In *Proc. of the 2013 American Control Conference*, 1189–1194.
- Markel, T., Brooker, A., Hendricks, T., Johnson, V., Kelly, K., Kramer, B., O’Keefe, M., Sprik, S., and Wipke, K. (2002). Advisor: A systems analysis tool for advanced vehicle modeling. *Journal of Power Sources*, 110(2), 255–266.
- MathWorks (2019). `intlinprog`: Mixed-integer linear programming. <https://www.mathworks.com/help/optim/ug/intlinprog.html>. (accessed 11-Nov.-2019).
- Mesbah, A. (2016). Stochastic model predictive control: An overview and perspectives for future research. *IEEE Control Systems Magazine*, 36(6), 30–44.
- Moura, S.J., Fathy, H.K., Callaway, D.S., and Stein, J.L. (2011). A stochastic optimal control approach for power management in plug-in hybrid electric vehicles. *IEEE Transactions on Control Systems Technology*, 19(3), 545–555.
- Nadaraya, E.A. (1964). On estimating regression. *Theory of Probability and its Applications*, 9(1), 141–142.
- Palmer Performance Engineering Corporation (2018). DashCommand™ for the iPhone or iPod Touch. <http://www.palmerperformance.com/products/dashcommand/>. (accessed 11-Nov.-2019).
- Pisu, P. and Rizzoni, G. (2007). A comparative study of supervisory control strategies for hybrid electric vehicles. *IEEE Transactions on Control Systems Technology*, 15(3), 506–518.
- Ripaccioli, G., Bernardini, D., Cairano, S.D., Bemporad, A., and Kolmanovsky, I.V. (2010). A stochastic model predictive control approach for series hybrid electric vehicle power management. In *Proc. of the 2010 American Control Conference*, 5844–5849.
- Sun, C., Moura, S.J., Hu, X., Hedrick, J.K., and Sun, F. (2015). Dynamic traffic feedback data enabled energy management in plug-in hybrid electric vehicles. *IEEE Transactions on Control Systems Technology*, 23(3), 1075–1086.
- Tamaki, S., Sakayanagi, Y., Sekiguchi, K., Ibuki, T., Tahara, K., and Sampei, M. (2014). On-line feedforward map generation for engine ignition timing control. *IFAC Proceedings Volumes*, 47(3), 5691–5696.
- Torres, J.L., Gonzalez, R., Gimenez, A., and Lopez, J. (2014). Energy management strategy for plug-in hybrid electric vehicles. a comparative study. *Applied Energy*, 113, 816–824.
- Toyota Motor Corporation (2016). Toyota Prius PHV. https://toyota.jp/pages/contents/priusphv/001_p_005/pdf/spec/priusphv_spec_201506.pdf. (accessed 11-Nov.-2019).
- Watson, G.S. (1964). Smooth regression analysis. *Sankhyā: The Indian Journal of Statistics, Series A (1961-2002)*, 26(4), 359–372.
- Wirasingha, S.G. and Emadi, A. (2011). Classification and review of control strategies for plug-in hybrid electric vehicles. *IEEE Transactions on Vehicular Technology*, 60(1), 111–122.